Journal of Power Sources 196 (2011) 5402–5407

Contents lists available at ScienceDirect

Journal of Power Sources

journal homepage: www.elsevier.com/locate/jpowsour

A graphene modified anode to improve the performance of microbial fuel cells

Yezhen Zhang[a], Guangquan Mo[a], Xuwen Li[a], Weide Zhang[a], Jiaqi Zhang[b], Jianshan Ye[a,*], Xiaodan Huang[c], Chengzhong Yu[d,**]

[a] School of Chemistry and Chemical Engineering, South China University of Technology, Guangzhou 510641, PR China
[b] School of Environmental Science and Safety Engineering, Tianjin University of Technology, Tianjin 300071, PR China
[c] Department of Chemistry and Shanghai Key Laboratory of Molecular Catalysis and Innovative Materials, Fudan University, Shanghai 200433, PR China
[d] ARC Centre of Excellence for Functional Nanomaterials and Australian Institute for Bioengineering and Nanotechnology, The University of Queensland, Brisbane, QLD 4072, Australia

ARTICLE INFO

Article history:
Received 23 January 2011
Accepted 20 February 2011
Available online 26 February 2011

Keywords:
Graphene
Biocatalyst
Microbial fuel cells

ABSTRACT

Graphene with a Brunauer–Emmett–Teller (BET) specific surface area of 264 $m^2 g^{-1}$ has been used as anodic catalyst of microbial fuel cells (MFCs) based on *Escherichia coli* (ATCC 25922). The electrochemical activities of plain stainless steel mesh (SSM), polytetrafluoroethylene (PTFE) modified SSM (PMS) and graphene modified SSM (GMS) have been investigated by cyclic voltammetry (CV), discharge experiment and polarization curve measurement. The GMS shows better electrochemical performance than those of SSM and PMS. The MFC equipped with GMS anode delivers a maximum power density of 2668 mW m^{-2}, which is 18 times larger than that obtained from the MFC with the SSM anode and is 17 times larger than that obtained from the MFC with the PMS anode. Scanning electron microscopy (SEM) results indicate that the increase in power generation could be attributed to the high surface area of anode and an increase in the number of bacteria attached to anode.

1. Introduction

Microbial fuel cells (MFCs) are novel electrochemical devices that directly convert microbial metabolic power into electricity using electrochemical technology, which have great potential in broad applications, such as wastewater treatment [1–4], implantable medical devices [5] and biosensors [6–8]. However, the low power density of MFCs remains one of the main obstacles for their practical applications [9,10]. Aside from all the other factors affecting the MFC performance, which include cell design, inoculum, substrate, proton exchange material and electrode surface areas, etc. [11–17], the fabrication materials of anode play a profound role in influencing the power generation by determining the actual accessible area for bacteria to anchor and affecting the interfacial electron transfer resistance. Therefore, a high-performance anode material is most essential to improve the power outputs of MFCs.

Traditionally, carbon materials such as carbon cloth, carbon paper, graphite granules and graphite felt tend to be suitable as anodes in MFCs due to their chemical stability, high conductivity and high specific surface area. However, the pores within such materials can be clogged by the entering bacteria, resulting in cell death and significant reduction of the electrochemical reaction surface [18], thus much decreased electrocatalytic activity for the electrode microbial reactions can be subsequently observed. Carbon nanotubes (CNTs) have also been explored to improve the power output of MFCs [19]. But CNTs have a cellular toxicity that could lead to proliferation inhibition and cell death [20,21].

Recently, graphene has been considered as the intriguing material, attracting strong scientific and technological interest with great application potentials in various fields, such as lithium ion batteries [22], solar cells [23] and electrochemical super-capacitors [24], for its unique nanostructure and extraordinary properties (high surface area [25], excellent conductivity [26], outstanding mechanical strength [27] and extraordinary electrocatalytic activities, etc.). Graphene can be synthesized by the chemical oxidation–reduction treatment of graphite [26,28,29], during which toxic metal catalysts are not used, which is a desired property for application in the MFCs. However, the application potential of graphene as an electrocatalyst material in MFCs has not been reported. In this study, the performance of a dual-chamber MFC operated with a graphene-modified stainless steel mesh (GMS) anode has been evaluated for the first time.

2. Experimental

2.1. Chemicals and materials

Polytetrafluoroethylene (PTFE) solution (1 wt.%) and 2-hydroxy-1,4-naphthoquinone (HNQ, 97%) were purchased from

* Corresponding author. Tel.: +86 20 87113241; fax: +86 20 87112901.
** Corresponding author. Tel.: +61 7 33463283; fax: +61 7 33463973.
E-mail addresses: jsye@scut.edu.cn (J. Ye), c.yu@uq.edu.au (C. Yu).

0378-7753/$ – see front matter © 2011 Elsevier B.V. All rights reserved.
doi:10.1016/j.jpowsour.2011.02.067

Sigma–Aldrich. Nafion 112 (Dupont, USA) was used as a cation exchange membrane. Graphene was obtained by the chemical oxidation–reduction treatment of graphite as described in our previous studies [30,31]. In a typical procedure, 5 g of graphite was slowly added into a stirred mixture of concentrated sulfuric (87.5 mL) and nitric acid (45 mL) in an ice-water bath. Subsequently, 55 g of $KClO_3$ was carefully added into the mixture. All the processes were carried out in the fume hood. It was kept stirring for 4 days at room temperature. Then 4 L of water was added to the slurry and the mixture was filtered to obtain graphite oxide. After dried at 80 °C, graphene oxide was exfoliated in de-ionized water by ultrasonic treatment for 2 h to form a colloidal graphene oxide suspension. Finally, the graphene oxide suspension reacted with hydrazine monohydrate (1 μL: 3 mg graphene oxide) for 24 h at 80 °C to obtain the graphene sheets. All other chemicals were from local chemical agent, and de-ionized water (>18.4 MΩ cm^{-1}) was used throughout.

2.2. Preparation of electrodes

Carbon paper (Hesen, China) and stainless steel mesh (SSM) were cut to small pieces with 1 cm × 1 cm. The pieces of carbon paper were treated by soaking in HCl (1.0 M), de-ionized water, NaOH (1.0 M) and de-ionized water sequentially. Each step of treatment was 1 h. The pieces of SSM were just soaked in HCl (1.0 M) for 1 h. After that, the small pieces were rinsed for several times and finally dried in oven at 60 °C for 12 h. These pretreated carbon papers were used as the cathodes for the MFCs.

5 mg of graphene powder was mixed with PTFE (1 wt.%) to form a paste. The paste was then coated on the surface of SSM to produce uniform films, followed by pressing with a presser to fabricate the GMS electrode. After drying at 60 °C to remove water, the electrode was used as the anode for the MFCs.

A control PTFE modified SSM (PMS) electrode was prepared using the same quantity of PTFE when prepared the GMS.

2.3. MFC construction and system set-up

As schematically shown in Fig. 1A, the MFC reactor was constructed using two round polymethylmethacrylate (PMMA) templates (Φ = 15 cm, 3 cm in thickness). The anodic or cathodic compartment was an inner cylinder (Φ = 9 cm, 2 cm in depth) in each template. The two compartments were screwed together and separated by two PMMA disc gaskets (Φ = 15 cm, 3 cm × 3 cm window in center) with Nafion 112 membrane (effective area of 9 cm^2). The MFC is shown in Fig. 1B.

Phosphate buffer solution (PBS) consisted of 10.0 g of $NaHCO_3$ and 8.5 g of NaH_2PO_4 per liter. Culture medium, which was a mixture of 10.0 g of peptone, 5.0 g of NaCl and 3.0 g of beef powder per liter, was sterilized in an autoclave (Sanshen Shanghai, China) at 120 °C for 20 min, and then placed in the incubator (Shenxian Shanghai, China) at 37 °C for 24 h before using. Original *Escherichia coli* (ATCC 25922, Guangdong Institute of Microbiology) biocatalyst was grown anaerobically in the prepared culture medium at 37 °C for 18–24 h. 5 mL of *Escherichia coli* culture was inoculated to anode (saturated with nitrogen for 20 min before inoculation). To evaluate the performance of anode, three MFCs with different anodes, namely SSM based MFC (MFC-SSM), PMS based MFC (MFC-PMS) and GMS based MFC (MFC-GMS) were set up simultaneously.

Anolyte was PBS containing 5 mmol of HNQ, 10.0 g of glucose and 5.0 g of yeast extract per liter. Catholyte was 50 mM $K_3[Fe(CN)_6]$. Both the volumes of anolyte and catholyte were 115 mL.

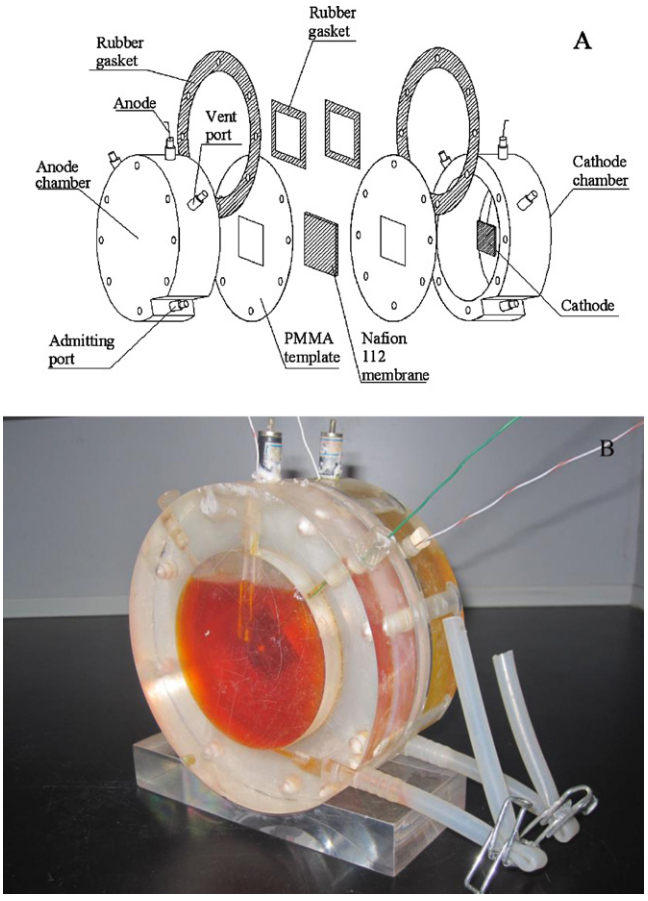

Fig. 1. Schematic (A) and photograph (B) of the dual-chamber MFC used in the experiment.

2.4. Characterization

The specific surface area of the sample was determined using Brunauer–Emmett–Teller (BET) method on a Quantachrome's Quadrasorb SI analyzer at 77 K. The morphology of graphene was characterized with scanning electron microscopy (SEM, LEO, Germany) at 25 kV. After discharge, the surface morphologies of the SSM, PMS and GMS were examined by a SE-30 EXEM SEM. The sample preparation was referred to the procedures described elsewhere [32]. Briefly, the samples (cut from the anodes) were fixed in 4% glutaraldehyde solution for more than 4 h to stabilize the bacteria attached to the anodes. Following a rinse in a PBS solution (pH 7.0) thrice, then the samples were dehydrated in ethanol series (50%, 70%, 80%, and 90%) for 10 min each and followed by 10 min changes in 100% ethanol twice. Further rinse was taken in isoamyl acetate twice (10 min each time). The samples were then dried at CO_2-critical point for 3 h.

2.5. Electrochemical measurements

All electrochemical experiments were performed on CHI660C (Chenhua, China) in a three-electrode arrangement, including a working electrode, a platinum counter electrode and an Ag/AgCl (saturated KCl) reference electrode. MFC characterization system (Ingsens Instrument, China) was used for data acquisition. For the determination of the power output, a variable resistance (0–10 kΩ) was used as the external load. Cell voltages were recorded at a time interval of 30 s across the external resistance and a controlled temperature of 35 °C.

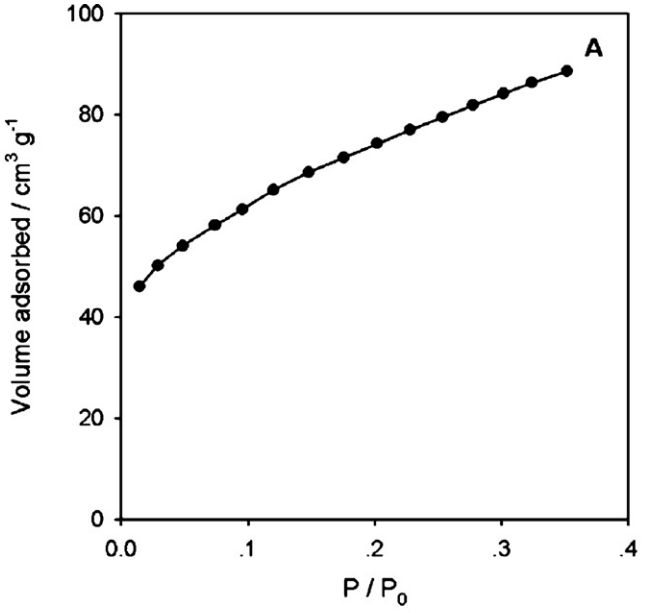

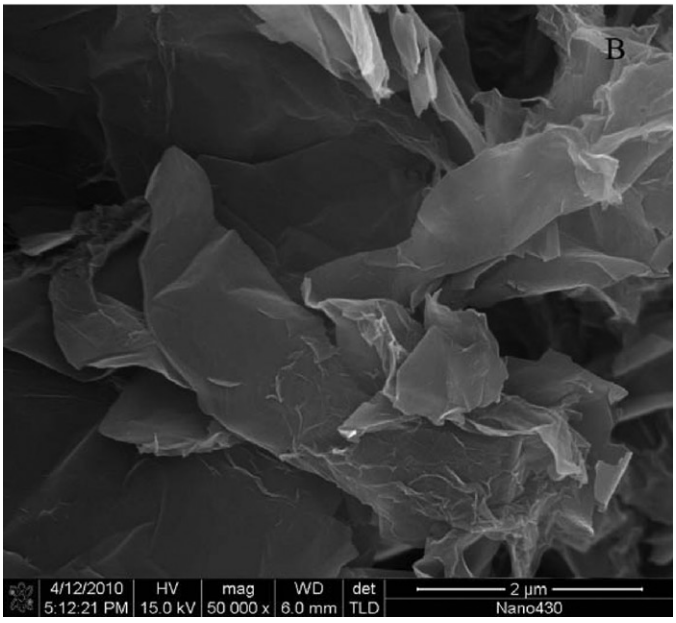

Fig. 2. Nitrogen adsorption isotherms (A) and SEM micrographs (B) of the graphene.

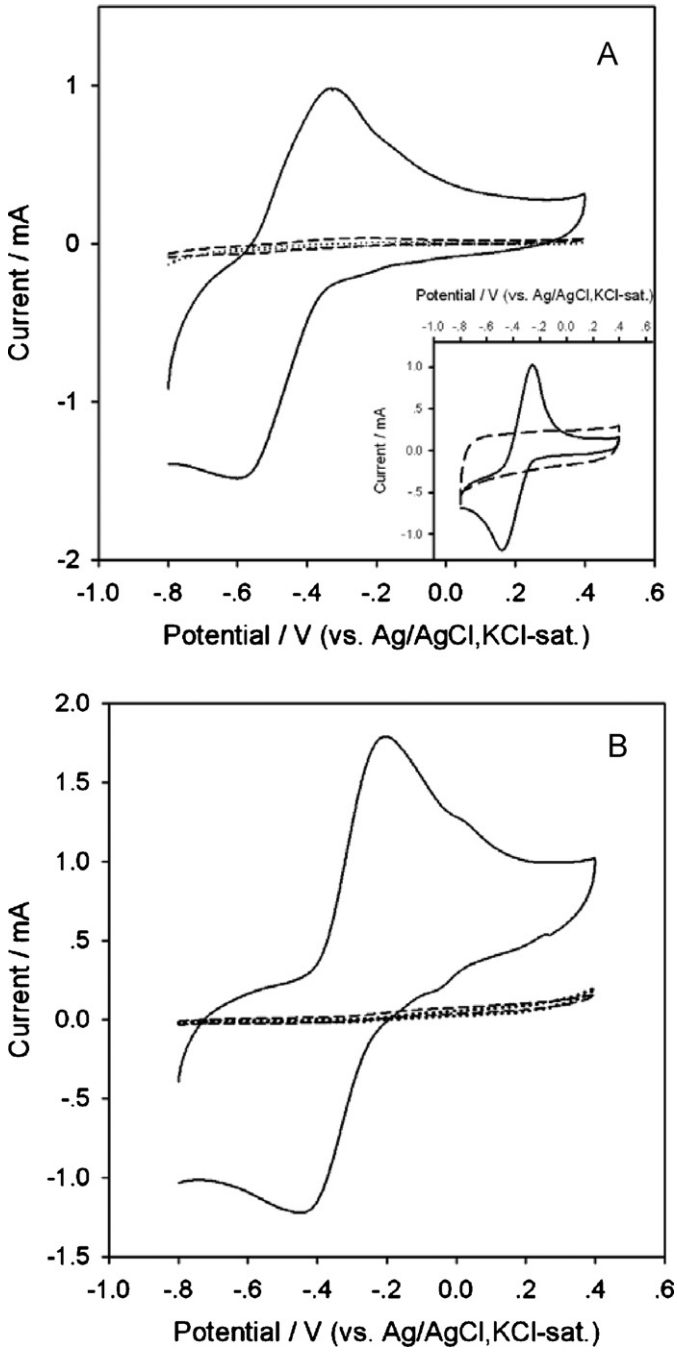

Fig. 3. CVs of SSM (long dash line), PMS (dotted line) and GMS (solid line) in anolyte without (A) and with (B) suspended cells of *E. coli* (ATCC 25922). The inset is the CVs of GMS in anolyte without HNQ (long dash line) and with HNQ (solid line). All the voltammograms were recorded with a scan rate of 10 mV s^{-1}.

3. Results and discussion

3.1. Characterization of graphene

The prepared graphene was characterized by nitrogen adsorption at 77 K (Fig. 2A). The BET specific surface area was calculated to be 264 m^2 g^{-1}, which was larger by about 500 times than that of woven graphite felt (about 0.5 m^2 g^{-1}) [32], a widely used anode material in MFCs. Fig. 2B shows the typical SEM image of the obtained graphene. The observed layered platelets composed of curled nanosheets are the representative morphology of graphene. The high surface area and excellent conductivity of graphene is expected to be beneficial for the bacteria to attach to the anode and enhance the charge transfer capability from the bacteria to the anode.

3.2. CV study

CV tests were carried out to determine the electrocatalytic behavior of anode materials. As revealed in Fig. 3A, GMS results in larger current responses when compared to SSM and PMS in the scan range between −0.8 V and 0.4 V in the absence of bacteria. This is a result of the enhanced surface area of GMS. The inset shows the CVs of GMS in anolyte with or without of HNQ. A set of redox peaks with a formal potential at −0.48 V indicates a typical reversible electron transfer reaction of the quinone group in HNQ to hydroquinone involving two electrons [33]. Fig. 3B shows the CVs of the SSM, PMS and GMS anodes after the inoculation of *Escherichia coli* in PBS solu-

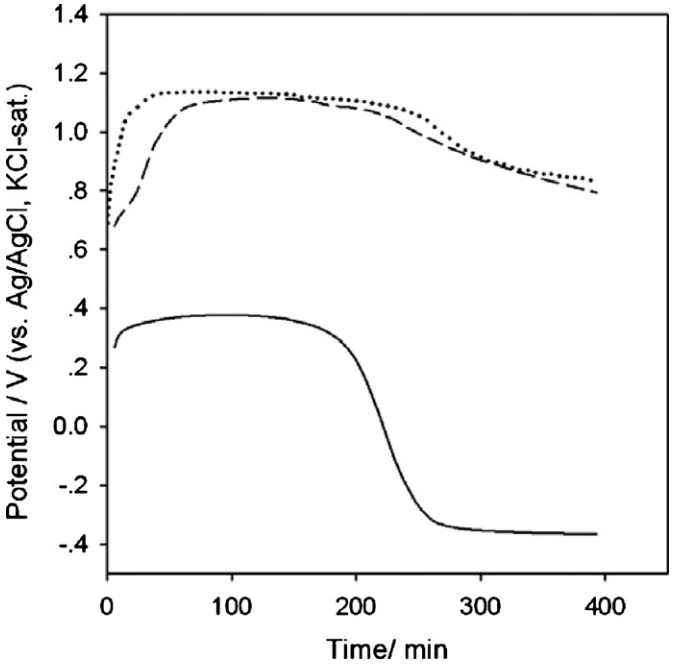

Fig. 4. Potential–time curves of MFCs utilizing SSM (long dash line), PMS (dotted line) and GMS (solid line).

tion. A peak current of 1.79 mA at −0.20 V in the oxidation scan and a peak current of −1.22 mA at −0.44 V in the reduction scan are observed at the GMS. The peak current is much higher than those at the SSM and PMS, which is due to the enhanced electron-transfer efficiency from the bacteria to the anode via graphene. The separation of the anodic and cathodic peak potentials (ΔE_p) is smaller than those at the SSM and PMS, indicating that graphene plays an important role in increasing the electroactive surface area [34]. The performances of SSM and PMS are similar, which shows the PTFE is just a bonder, which does not contribute to the power output much.

3.3. Anode discharge performance in MFC

In order to evaluate the discharge performance of different anodes, the constant-current discharge experiments of MFCs with three different anodes in 5 mM glucose solution were conducted at 0.01 mA cm^{-2}, resulting in a change of the anode potential versus the discharge time as shown in Fig. 4. The anodic potential versus time data showed different discharge profiles for the three anodes. For the SSM anode, it has a very high polarization potential of 1.1 V initially, and gradually becomes lower. Finally, it reaches at 0.79 V. For the PMS anode, it also has a very high polarization potential of 1.1 V initially, and gradually becomes lower. Finally, it reaches at 0.83 V. For the GMS anode, it has a polarization potential of about 0.35 V at the beginning, and gradually becomes lower with increasing discharge time and finally becomes constant at its lowest polarization potential of −0.37 V. For an anodic reaction, the more negative the anode discharge potential, the better the electrocatalytical performance. Apparently, the GMS gives the most negative potential in the three electrodes during the discharge process, demonstrating that it has better electrocatalytic performance than SSM and PMS, which is in agreement with the CV result in Fig. 3.

3.4. Power generation

The dual-chamber MFC operated with the GMS anode generated substantially larger power densities compared to the SSM and PMS

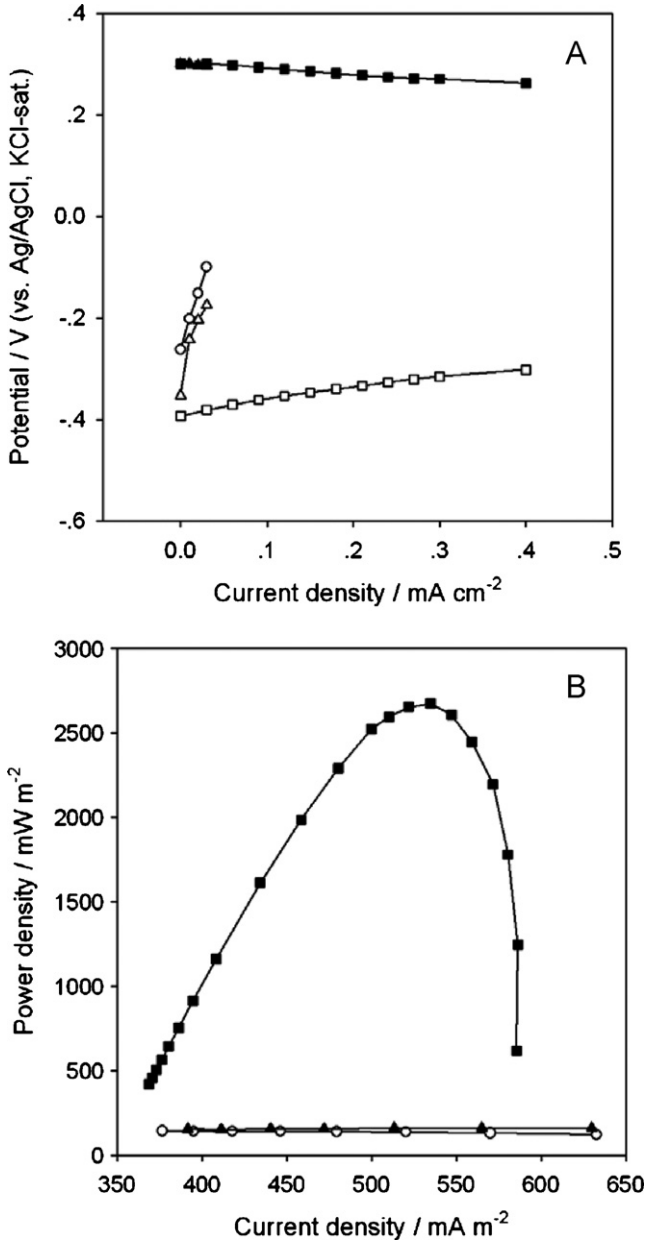

Fig. 5. Power generation properties of MFCs operated with the SSM (circle), PMS (triangle) and GMS (square): (A) anode (open symbol) and cathode (filled symbol) polarization curves and (B) power density curves of three MFCs.

counterpart. Anode and cathode polarization curves of the three MFCs were separately obtained, as shown in Fig. 5A. The catholyte was a 50 mM ferricyanide solution with PBS identical to that in the bacterial medium. Using ferricyanide as the electron acceptor here is owing to its facile reaction rate [35,36], so there are insignificant differences in cathode polarization behavior for the three MFCs with the same cathode material. However, the anode polarization curves are significantly different. A sharp decrease in the slope of the anode polarization curve is observed in MFC-GMS versus in MFC-SSM and MFC-PMS. For the MFC-SSM and MFC-PMS, increasing current densities from 0 to 0.03 mA cm^{-2} caused a significant rise in the anode potential from −0.26 V (MFC-SSM) and −0.35 V (MFC-PMS) to −0.10 V (MFC-SSM) and −0.17 V (MFC-PMS). This indicates that a large driving force (in the form of overpotential) is required for the bio-electrochemical reaction at high currents. However, for the MFC-GMS, the anode polarization is significantly smaller as the anode potential changed from −0.39 V to −0.30 V

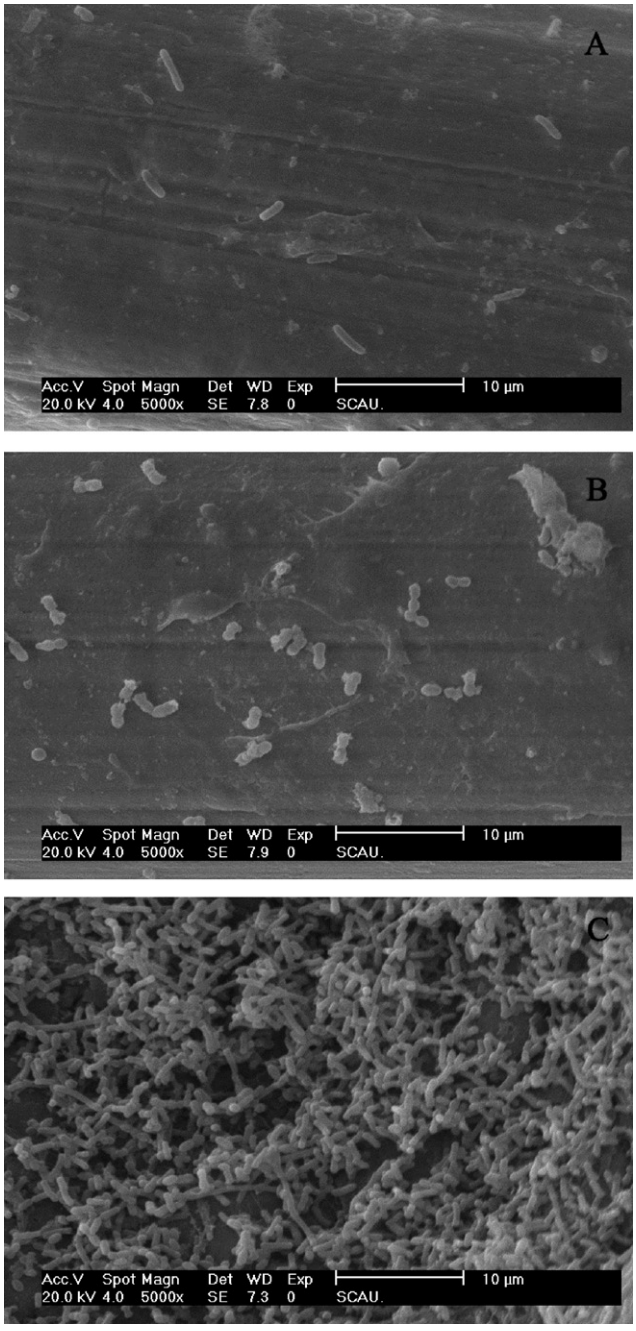

Fig. 6. SEM micrographs of *E. coli* cells adhered on SSM (A), PMS (B) and GMS (C).

with the increase of current density from 0 to 0.30 mA cm^{-2}. These results are the consequence of an enhanced anode performance by increasing the anode surface area and the biocompatibility of the substrate. Fig. 5B shows power density curves of the three MFCs investigated. The maximum power density of the MFC-GMS is 2668 mW m^{-2}, which increased by 18 times as compared with that (142 mW m^{-2}) produced from the MFC-SSM and by 17 times as compared with that (159 mW m^{-2}) produced from the MFC-PMS. The results substantially demonstrate that the graphene can be a superior anode material with high power output in MFCs.

3.5. SEM study

After discharge, the surface morphologies of each electrode were immediately examined by SEM. The grown bacteria on the electrodes exhibited a rod-shaped structure, which is similar to the literature [37]. The SSM and PMS electrodes possess relatively smooth surfaces. Only a few bacteria are observed to be attached on the electrodes (Fig. 6A and B). But the GMS electrode possesses a rough and large surface. Lots of *Escherichia coli* cells accumulate on the electrode surface and adhere to one another (Fig. 6C). This result indicates that GMS can promote bacteria adhesion on the anode surface, which plays a key role in improving the power output.

4. Conclusions

The GMS system gives a much higher power output than those of SSM and PMS. Because it can improve surface area of electrode, adhesion of bacteria and efficiency of electron transfer. These results provide significant prospects for developing low cost and effective anode of MFCs. Further studies are necessary to assess whether GMS can be applicable to large-scale MFCs from a practical perspective.

Acknowledgements

The authors gratefully acknowledge the financial support of the 863 Program (2008AA06Z311) and NSFC (20945004).

References

[1] B.E. Logan, Water Sci. Technol. 52 (2005) 31–37.
[2] R.A. Rozendal, H.V.M. Hamelers, K. Rabaey, J. Keller, C.J.N. Buisman, Trends Biotechnol. 26 (2008) 450–459.
[3] J. Sun, Y.Y. Hu, Z. Bi, Y.Q. Cao, J. Power Sources 187 (2009) 471–479.
[4] S. Young-Chae, Y. Kyu Seon, L. Song Kuen, J. Power Sources 195 (2010) 6478–6482.
[5] Y. Han, C. Yu, H. Liu, Biosens. Bioelectron. 25 (2010) 2156–2160.
[6] I.S. Chang, J.K. Jang, G.C. Gil, M. Kim, H.J. Kim, B.W. Cho, B.H. Kim, Biosens. Bioelectron. 19 (2004) 607–613.
[7] I.S. Chang, H. Moon, J.K. Jang, B.H. Kim, Biosens. Bioelectron. 20 (2005) 1856–1859.
[8] J.M. Tront, J.D. Fortner, M. Plotze, J.B. Hughes, A.M. Puzrin, Biosens. Bioelectron. 24 (2008) 586–590.
[9] D.C. Holzman, Environ. Health Perspect. 113 (2005) A754–A757.
[10] R.A. Bullen, T.C. Arnot, J.B. Lakeman, F.C. Walsh, Biosens. Bioelectron. 21 (2006) 2015–2045.
[11] H.S. Park, B.H. Kim, H.S. Kim, H.J. Kim, G.T. Kim, M. Kim, I.S. Chang, Y.K. Park, H.I. Chang, Anaerobe 7 (2001) 297–306.
[12] G.-C. Gil, I.-S. Chang, B.H. Kim, M. Kim, J.-K. Jang, H.S. Park, H.J. Kim, Biosens. Bioelectron. 18 (2003) 327–334.
[13] S.E. Oh, B.E. Logan, Appl. Microbiol. Biotechnol. 70 (2006) 162–169.
[14] A. Thygesen, F.W. Poulsen, B. Min, I. Angelidaki, A.B. Thomsen, Bioresour. Technol. 100 (2009) 1186–1191.
[15] Y. Mohan, D. Das, Int. J. Hydrogen Energy 34 (2009) 7542–7546.
[16] C.S. Butler, R. Nerenberg, Appl. Microbiol. Biotechnol. 86 (2010) 1399–1408.
[17] N. Joo-Youn, K. Hyun-Woo, S. Hang-Sik, J. Power Sources (2010) 6428–6433.
[18] K. Rabaey, W. Verstraete, Trends Biotechnol. 23 (2005) 291–298.
[19] H.Y. Tsai, C.C. Wu, C.Y. Lee, E.P. Shih, J. Power Sources 194 (2009) 199–205.
[20] E. Flahaut, M.C. Durrieu, M. Remy-Zolghadri, R. Bareille, C. Baquey, J. Mater. Sci. 41 (2006) 2411–2416.
[21] A. Magrez, S. Kasas, V. Salicio, N. Pasquier, J.W. Seo, M. Celio, S. Catsicas, B. Schwaller, L. Forr, Nano Lett. 6 (2006) 1121–1125.
[22] E. Yoo, J. Kim, E. Hosono, H.-S. Zhou, T. Kudo, I. Honma, Nano Lett. 8 (2008) 2277–2282.
[23] X. Wang, L. Zhi, K. Mullen, Nano Lett. 8 (2007) 323–327.
[24] S.R.C. Vivekchand, C.S. Rout, K.S. Subrahmanyam, A. Govindaraj, C.N.R. Rao, J. Chem. Sci. 120 (2008) 9–13.
[25] M.J. McAllister, J.L. Li, D.H. Adamson, H.C. Schniepp, A.A. Abdala, J. Liu, M. Herrera-Alonso, D.L. Milius, R. Car, R.K. Prud'homme, I.A. Aksay, Chem. Mater. 19 (2007) 4396–4404.
[26] A.K. Geim, K.S. Novoselov, Nat. Mater. 6 (2007) 183–191.
[27] C. Lee, X.D. Wei, J.W. Kysar, J. Hone, Science 321 (2008) 385–388.
[28] S. Stankovich, D.A. Dikin, R.D. Piner, K.A. Kohlhaas, A. Kleinhammes, Y. Jia, Y. Wu, S.T. Nguyen, R.S. Ruoff, Carbon 45 (2007) 1558–1565.
[29] S. Stankovich, R.D. Piner, X.Q. Chen, N.Q. Wu, S.T. Nguyen, R.S. Ruoff, J. Mater. Chem. 16 (2006) 155–158.

[30] H.J. Du, J.S. Ye, J.Q. Zhang, X.D. Huang, C.Z. Yu, Electroanalysis 22 (2010) 2399–2406.
[31] N. Li, M. Zhu, M. Qu, X. Gao, X. Li, W. Zhang, J. Zhang, J. Ye, J. Electroanal. Chem. 651 (2011) 12–18.
[32] D.H. Park, J.G. Zeikus, Biotechnol. Bioeng. 81 (2003) 348–355.
[33] S.A. Lee, Y. Choi, S.H. Jung, et al., Bioelectrochemistry 57 (2002) 173–178.
[34] Y.J. Zou, C.L. Xiang, L.N. Yang, L.X. Sun, F. Xu, Z. Cao, Int. J. Hydrogen Energy 33 (2008) 4856–4862.
[35] S. Oh, B. Min, B.E. Logan, Environ. Sci. Technol. 38 (2004) 4900–4904.
[36] L.X. Zhang, S.G. Zhou, L. Zhuang, W.S. Li, J.T. Zhang, N. Lu, L.F. Deng, Electrochem. Commun. 10 (2008) 1641–1643.
[37] Y. Qiao, S.J. Bao, C.M. Li, X.Q. Cui, Z.S. Lu, J. Guo, ACS Nano 2 (2008) 113–119.